0026-895X/97/030437-08$3.00/0

MOLECULAR PHARMACOLOGY, **52:**437–444 (1997).

Inhibition of Mitosis and Microtubule Function through Direct Tubulin Binding by a Novel Antiproliferative Naphthopyran LY290181

DAN L. WOOD, DULAL PANDA, TODD R. WIERNICKI, LESLIE WILSON, MARY ANN JORDAN, and JAI PAL SINGH

Cardiovascular Research, Lilly Research Laboratories, Indianapolis, Indiana 46285 (D.L.W., T.R.W., J.P.S.), and Department of Molecular, Cellular, and Developmental Biology, University of California, Santa Barbara, California 93106 (D.P., L.W., M.A.J.)

Received February 10, 1996; Accepted May 15, 1997

SUMMARY

The mechanism of action of a novel antiproliferative compound LY290181 [2-amino-4-(3-pyridyl)-4*H*-naphtho(1,2-b)pyran-3-carbonitrile] was characterized. LY290181 is a potent inhibitor of cell proliferation, producing 50% inhibition of vascular smooth muscle, endothelial, Chinese hamster ovary, HeLa, and human erythroleukemia cells at concentrations of 8–40 nM. Cell cycle analysis showed that LY290181 caused accumulation of smooth muscle cells at the G_2/M phase and induced mitotic arrest in Chinese hamster ovary cells and HeLa cells. At low concentrations (3–30 nM), LY290181 blocked transition of cells from metaphase to anaphase and disrupted mitotic spindle organization. At high concentrations (≥100 nM), LY290181 produced a concentration-dependent loss of cytoplasmic and spindle microtubules. LY290181 inhibited the polymerization of purified bovine brain microtubule protein into microtubules, and it depolymerized preformed microtubules. Using tubulin-1-anilino-8-naphthalene sulfonate complex fluorescence, we have shown that LY290181 directly interacted with tubulin in a unique manner. These studies show that LY290181 induces cell growth arrest in prometaphase/metaphase, and tubulin appears to be its molecular target.

Proliferation of vascular smooth muscle cells plays an important role in the pathogenesis of vascular disease including atherosclerosis (1), transplant atherosclerosis (2), restenosis (1–3), hypertension (4), renal disease (5), and diabetic arteriopathy and retinopathy (6). Animal model studies have demonstrated that arterial intimal thickening after vascular injury can be suppressed by inhibitors of smooth muscle cell proliferation. Direct application of specific cell growth inhibitors such as toxin-conjugated growth factor (7) or antisense to cell cycle regulatory genes (8, 9) have been shown to produce a dramatic reduction in intimal thickening in balloon-injured rat carotid arteries. Our recent studies have shown that the naphthopyran LY290181 [2-amino-4-(3-pyridyl)-4*H*-naphtho(1,2-b)pyran-3-carbonitrile] is a novel antiproliferative compound that inhibits vascular smooth muscle cell proliferation (10). LY290181 also produced a substantial inhibition of intima thickening in a rat carotid artery injury model when administered systemically (10). Recent studies have also shown that LY290181 and its structural analogs inhibit the synthesis and secretion of metalloproteinases from chondrocytes (11). LY290181 was also found to reduce diabetes-induced endothelial cell dysfunction including, blood flow and vascular permeability (12). The mechanism of cell growth inhibition or other cellular activities of LY290181 is not understood. We recently found that LY290181 kinetically stabilized microtubule growth and shortening dynamics, apparently by binding to a unique site in tubulin (13). In the present study we have investigated the antiproliferative activity, the stage of cell cycle arrest, and the molecular target for the antiproliferative action of LY290181. We show here that LY290181 is a potent antimitotic agent whose antiproliferative activity is apparently mediated by binding to tubulin and modulation of microtubule function.

Experimental Procedures

Cell cultures. Primary cultures of rabbit aortic vascular smooth muscle cells were prepared from New Zealand White rabbits as described previously, and used at passages 2 through 4. The smooth muscle cells were cultured in growth medium consisting of DMEM, 10% FBS, L-glutamine (2 mM), penicillin (100 units/ml), and streptomycin (100 μg/ml) (Life Technologies, Grand Island, NY). CHO and

This work was supported in part by National Institute of Neurological Disorders and Stroke Grant NS13560.

ABBREVIATIONS: DMEM, Dulbecco's modified Eagle's medium; FBS, fetal bovine serum; FACS, fluorescence-activated cell sorting; FITC, fluorescein isothiocyanate, BSA, bovine serum albumin; MAP, microtubule-associated protein; PBS, phosphate-buffered saline; ANS, 1-anilino-8-naphthalene sulfonate; CHO, Chinese hamster ovary; PEG, polyethylene glycol; PIPES, 1,4-piperazinediethanesulfonic acid; EGTA, ethylene glycol bis(β-aminoethyl ether)-*N*,*N*,*N*′,*N*′-tetraacetic acid.

human erythroleukemia cell lines were obtained from American Type Culture Collection and grown in Ham's F-12 medium containing 10% FBS, 2 mM L-glutamine, 100 units/ml penicillin, and 100 μg/ml streptomycin. Human umbilical vein endothelial cells were from Clonetics (San Diego, CA).

Cell proliferation assay. Smooth muscle cell proliferation was determined using third passage rabbit aortic smooth muscle cells that were seeded into 24-well plates at a starting density of 1×10^4 cells/well in growth medium. The cells were allowed to adhere at 37° under 5% CO_2 and 95% air for 16 hr. The medium was then replaced with DMEM containing 10% FBS and the indicated concentrations of LY290181. After a 72-hr incubation, cells were trypsinized and counted using a ZM Coulter Counter (Coulter Electronics, Miami Lake, FL).

Cell cycle analysis. Primary cultures of rabbit aortic smooth muscle cells were plated at 100,000 cells/well in six-well plates in growth medium as described above. After 24 hr, 30 or 100 nM LY290181 was added to the cultures. After 40 hr, attached cells were trypsinized and combined with those in the supernatant. Cells were washed twice in DMEM and fixed by resuspending in 1 ml of 70% methanol for 2 min at room temperature. Cells were pelleted at $3000 \times g$ for 5 min, resuspended in 1 ml of 0.1% Triton X-100 in PBS, and incubated at room temperature for 15 min. Cell suspensions were centrifuged as above and then resuspended in 0.5 ml of 50 mg/ml propidium iodide solution in PBS containing 200 μg/ml of RNase A. Cells were stored overnight at 4°. DNA content was determined by flow cytometry. The results were analyzed using the Modfit cell cycle analysis program (Varity Software, Topshan, NE).

Determination of mitotic index. CHO cells were plated on coverslips in six-well plates at 60,000 cells/well, and allowed to attach overnight in F-12 medium. Cells were then treated with the indicated concentrations of LY290181 for 8 hr. The medium was aspirated, and cells were stained with Diff Quick (Baxter, Miami, FL). Cells were mounted on the tissue culture plate with aqueous mounting medium and cover slips. The mitotic index was determined by counting interphase and mitotic cells at a magnification of 40× using a Nikon Diaphot inverted microscope. At least 1000 cells per data point were counted.

Immunofluorescence microscopy. Collagen-coated coverslips were prepared by incubating the coverslips with rat tail type I collagen (50 mg/ml in 0.02 N acetic acid) for 1 hr at room temperature followed by washing with PBS. CHO cells were plated on the coverslips in six-well plates at 60,000 cells/well, and allowed to attach overnight in F-12 medium. Cells were then treated with the indicated concentrations of LY290181 for 20 hr. The medium was aspirated gently, and the cells were fixed in polyethylene glycol and formaldehyde as described previously (14). Briefly, cells were covered with 2 ml of PEM/PEG buffer consisting of 80 mM PIPES, 1 mM EGTA, 1 mM $MgCl_2$, pH 7.1, and 40 g/liter PEG-8000. After 1 min, the buffer was aspirated, and cells were covered with 1 ml of 0.5% Triton X-100 in PEM (80 mM PIPES, 1 mM EGTA, 1 mM $MgCl_2$, pH 7.1) for 1 min followed by another 1-min incubation in PEM/PEG buffer. After removing the PEM/PEG buffer, the cells were covered with 3% formaldehyde in PEM for 20 min at room temperature. The formaldehyde was then removed, and the cells were washed once in PBS and stored at 4°. Fixed cells were stained by FITC-conjugated monoclonal anti-β-tubulin antibodies (1 mg/ml in PBS containing 1% BSA). After tubulin staining, DNA was stained with 1 mg/ml propidium iodide in PBS containing 1% BSA. Coverslips were mounted on slides in 0.1% *p*-phenylenediamine in PBS:glycerol (1:9). Slides were photographed and counted on a Nikon Microphot FXA at 60× magnification. Treatments were performed in duplicate and counted as blinded samples with a minimum of 1500 cells/slide. HeLa cell culture, determination of proliferation, and immunofluorescence microscopy after 20 hr of incubation with the compound were carried out as described previously (15).

Purification of microtubule protein and tubulin. Bovine brain microtubule protein consisting of ~70% tubulin and 30% MAPs was isolated without glycerol by three cycles of polymerization and depolymerization (16). Tubulin was purified from the microtubule protein preparation by phosphocellulose chromatography (16). The tubulin solution was quickly frozen as drops in liquid nitrogen and stored at −70° until used. The protein concentration was determined by the method of Bradford using a BSA standard.

Inhibition of microtubule polymerization by LY290181. Microtubule protein (1.2 mg/ml) was mixed with different concentrations of LY290181 in 100 mM PIPES, 1 mM $MgCl_2$, and 1 mM EGTA (100 mM PEM buffer), and 1 mM guanosine 5′-triphosphate. Microtubule polymerization was monitored at 37° by light scattering at 350 nm using a Gilford Response Spectrophotometer. The plateau absorbance values were used for calculations.

Fluorometric titration. The interaction of LY290181 with tubulin was monitored by its effects on the intrinsic fluorescence of tubulin-ANS complex (17, 18). Relative fluorescence intensities were obtained with a Perkin-Elmer LS50B spectrophotometer at 34° using a constant temperature water circulating bath. Buffer blank values were subtracted from all measurements. A tubulin concentration of 2 μM was used for all measurements. The excitation and emission wavelengths were 400 and 468 nm, respectively. We used 400 nm as the excitation wavelength to avoid any inner filter effect at high drug concentrations. LY290181 (10 μM) by itself had very low absorbance of 0.011 at 400 nm.

Materials. LY290181 was synthesized at the Eli Lilly Research Laboratories (10). The compound was prepared in dimethyl sulfoxide as a 10 mM stock solution and diluted in culture medium to the indicated concentrations. Recombinant human platelet-derived growth factor-BB was obtained from Genzyme (Cambridge, MA). Rat tail collagen was obtained from Collaborative Research (Bedford, MA). Anti-tubulin antibodies KXM-1 clone were obtained from Boehringer Mannheim (Indianapolis, IN).

Results

Antiproliferative activity of LY290181. LY290181 (Fig. 1) produced a concentration-dependent inhibition of vascular smooth muscle cell proliferation. The concentration of LY290181 required for IC_{50} of vascular smooth muscle cell proliferation was 20 nM. Similar results were obtained with human umbilical vein endothelial cells (IC_{50} = 20 nM), CHO cells (IC_{50} = 35 nM), human erythroleukemia cells (IC_{50} = 40 nM), and HeLa cells (IC_{50} = 8 nM). These data showed that LY290181 is a potent antiproliferative agent for a variety of cell types.

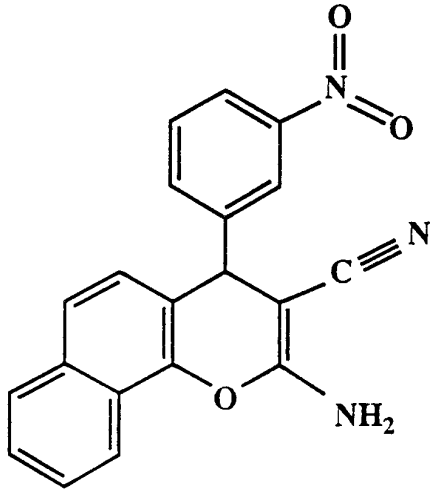

Fig. 1. Structure of LY290181.

Effects of LY290181 on progression through G_2/M. Rabbit aortic smooth muscle cells were plated at 100,000 cells/well in six-well plates and then treated with 30 or 100 nM LY290181 for 40 hr. FACS analysis (Fig. 2) shows that LY290181 produced a concentration-dependent accumulation of cells in the G_2/M phase of the cell cycle. In the presence of 30 nM LY290181, 28.9% of the cells accumulated in G_2/M, compared with 16.8% in controls. The fraction of cells in G_2/M increased to 68.6% at 100 nM LY290181. Correspondingly, the fraction of cells in G_0/G_1 was reduced from 74.3 to 62.1% at 30 nM LY290181, and to 22.9% at 100 nM LY290181.

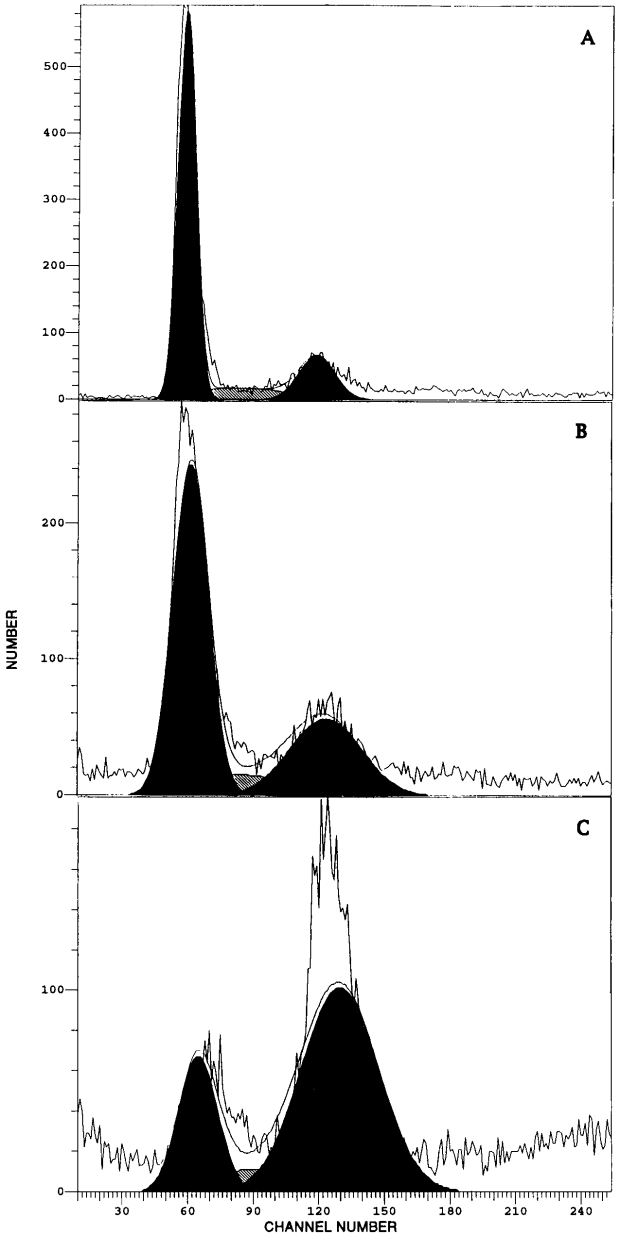

Fig. 2. Effect of LY290181 on cell cycle progression. Rabbit aortic smooth muscle cells were plated in growth medium in six-well plates at a density of 1×10^4 cells/well. The cultures were then treated with vehicle (A), 30 nM LY290181 (B), or 100 nM LY290181 (C) for 40 hr. Cells were then processed for propidium iodide staining and FACS analysis. Cell distribution in G_0/G_1, S, and G_2/M, was determined using the Varity Modfit program. The areas under the *left solid peak*, the *middle shaded peak*, and the *right solid peak* represent fraction of cells in G_0/G_1, S, and G_2/M, respectively.

These results show that, in cultures of cycling smooth muscle cells, LY290181 arrests cell cycle progression in G_2/M.

Mitotic arrest of CHO cells by LY290181. To further determine whether LY290181 inhibited cell cycle progression in G_2 or mitosis, cycling CHO cells were treated with the indicated concentrations of LY290181 for 8 hr, and mitotic indices in control and LY290181-treated cells were determined. The effect of LY290181 on CHO cell proliferation after 20 hr of incubation was also determined in parallel experiments. LY290181 produced a concentration-dependent increase in the mitotic index in CHO cells (Fig. 3). The effective concentrations paralleled those required for the inhibition of cell proliferation (Fig. 3, *inset*). Thus, LY290181 blocks CHO cells in mitosis.

LY290181 blocks cells in prometaphase/metaphase and produces a loss of interphase microtubules. To identify the subcellular target for LY290181, we examined its effect on the organization of chromosomes and microtubules during mitosis. CHO cells were grown on collagen-coated coverslips and then treated with varying concentrations of LY290181 for 20 hr. Chromosomal organization was determined after DNA staining with propidium iodide. In control cultures, nuclear staining with propidium iodide revealed a spectrum of mitotic figures including cells in metaphase and telophase of mitosis (Table 1). In cultures treated with 30 nM LY290181, 2.1 ± 0.2% of the cells were accumulated in prometaphase as compared with 1.1 ± 0.4% in the control (Table 1). At this concentration, metaphase and telophase figures were still present. At higher concentrations of LY290181, a concentration-dependent accumulation of prometaphase or "C-mitotic" figures was observed with a concomitant loss of

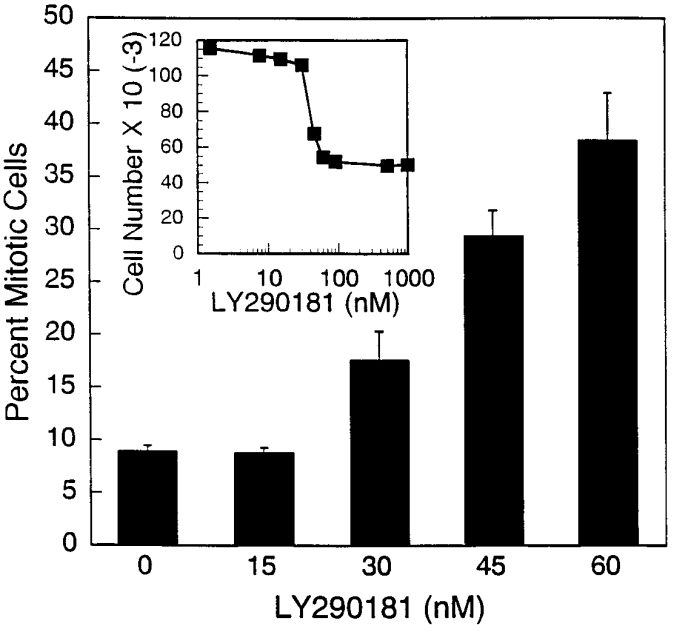

Fig. 3. Effect of LY290181 on mitotic arrest in CHO cells. CHO cell cultures in log phase of growth were treated with the indicated concentrations of LY290181 for 8 hr. Cells were then fixed and stained with Diff Quick. Mitotic indices were determined by counting interphase and mitotic cells at 40× magnification using a Nikon Diaphot inverted microscope. At least 1000 cells per data point were counted. Data are presented as mean ± standard deviation ($n = 3$). Cell proliferation (*inset*) under identical treatments was determined by cell counting after 20 hr of incubation.

TABLE 1

Effect of LY290181 on mitosis in CHO cells

Cells were grown on collagen coated coverslips, and treated with the indicated concentrations of LY290181 for 20 hr. Cells were then stained with propidium iodide and counted for distribution in various phases of the cell cycle. At least 1500 cells on each slide were counted. Values are mean ± SD (n = 3).

LY290181	Inter	Pro/Prometa	Meta	Ana/Telo
nM		%		
0	95.0 ± 0	1.1 ± 0.4	1.5 ± 0.3	2.3 ± 0.07
15	94.5 ± 0.7	0.97 ± 0.3	1.6 ± 0.5	3.2 ± 0.2
30	95.5 ± 0.7	2.1 ± 0.2	0.6 ± 0	1.9 ± 0.2
45	87.0 ± 4.2	13 ± 4.7	0.2 ± 0.3	0.3 ± 0.07
60	54.0 ± 24	46 ± 24	0	0

Inter, interphase; Pro, prophase, Prometa, prometaphase; Meta, metaphase; Ana, anaphase; Telo, telophase.

metaphase and telophase cells. The mitotic index as determined by the fraction of rounded cells after drug treatment is a less specific method with relatively high background level of rounded cells than the chromosomal morphology method for the determination of cells in mitosis. Although both methods provided qualitatively similar results, the chromosomal morphology methods provided more accurate quantitative data for accumulation of cells in mitosis and the stage of cell cycle block. These results indicate that the predominant action of LY290181 is to block cell cycle progression at prometaphase/metaphase.

We also determined the organization of interphase cytoplasmic microtubules after treatment with LY290181 by staining CHO cells with FITC-conjugated β-tubulin antibody. As shown in Fig. 4, at 30 nM LY290181, a concentration that produce 50% inhibition of cell proliferation, microtubules were still present in interphase cells, and the density and organization of the microtubules were not grossly altered. Higher concentrations of LY290181 produced a clear concentration-dependent loss of cytoplasmic microtubules; for example, cytoplasmic microtubule staining was nearly abolished at 500 nM LY290181. Unlike the actions of vinblastine or Taxol at high concentrations, tubulin paracrystal formation or microtubule bundling was not observed at high concentrations of LY290181.

Effect of LY290181 on mitotic spindle organization. Incubation of HeLa cells with LY290181 for 20 hr induced a block in mitosis at the transition from metaphase to anaphase. Fifty percent of the cells were blocked in metaphase at 10 nM LY290181, and the block was maximum (79%) at 30 nM LY290181. Concomitant with the increase in cells in metaphase, the proportion of cells in anaphase was decreased. Thus, in control cultures the ratio of cells in anaphase to cells in metaphase was 0.20, whereas the ratio decreased to 0.11 at 3 nM, to 0.01 at 10 nM, and no anaphase figures were observed at ≥30 nM LY290181.

As shown in Fig. 5, A and B, in control cells the metaphase spindles were bipolar and contained a compact equatorial plate of condensed chromosomes. At 3 nM LY290181, the organization of many spindles (43%) was abnormal. As shown in Fig. 5, C and D, abnormal spindles were bipolar but contained from one to several chromosomes that had not congressed to the metaphase plate; these uncongressed chromosomes were located at or near the spindle poles. Block in prometaphase/metaphase was accompanied by further distortion in the organization of the spindle microtubules and chromosomes. At 10 nM LY290181, 97% of the spindles were

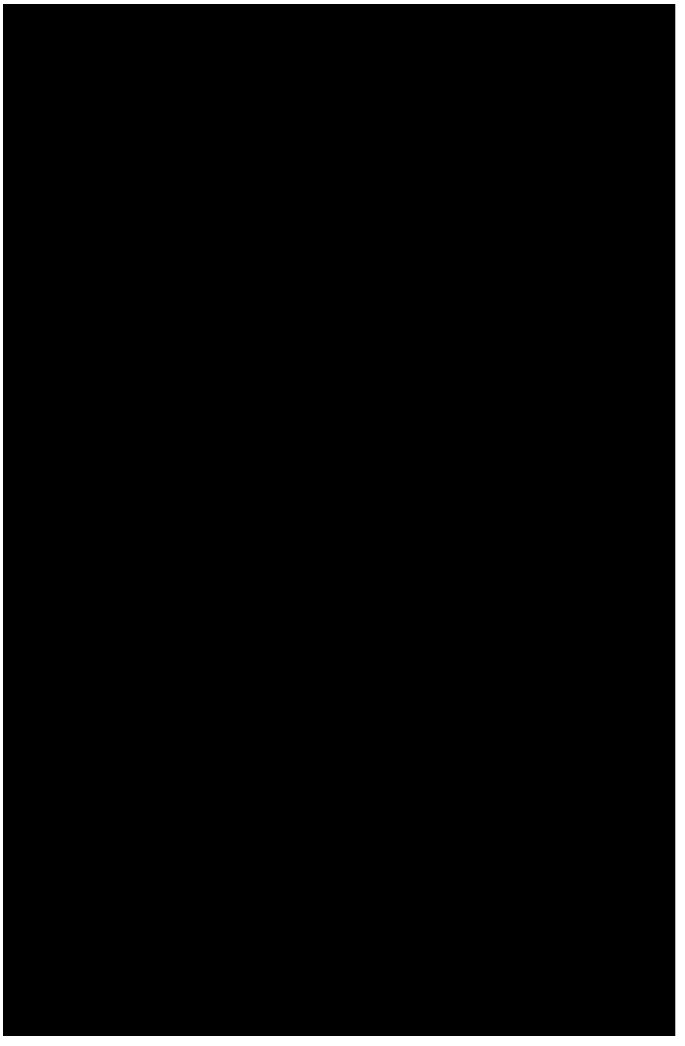

Fig. 4. Effect of LY290181 on microtubules in CHO cells. CHO cells were plated on collagen-coated coverslips. After 16 hr, cells were treated with vehicle (A), 30 nM (B), 60 nM (C), 90 nM (D), or 500 nM (E) LY290181. Cells were then fixed, and microtubules were stained with FITC-conjugated tubulin antibody. Cells were photographed at 60× magnification.

abnormal. Abnormal spindles consisted of three types, 1) bipolar containing uncongressed chromosomes, 2) monopolar "C-mitosis," 3) tripolar or multipolar (Fig. 5, E and F). At >30 nM LY290181, 100% of the spindles were abnormal and monopolar in organization. The mass of microtubules in mitotic and interphase cells did not appear reduced at 10 nM LY290181. However, at 30 nM LY290181 the microtubules of mitotic spindles were shorter and lower in number then microtubules in the control spindles, and the spindles appeared as numerous compact and small star-shaped structures (Fig. 5, G and H). In contrast, microtubules of interphase HeLa cells were not significantly affected at 30 nM LY290181 (data not shown). However, at higher drug concentrations (≥100 nM), both mitotic and interphase microtubules were lost. Thus at antiproliferative concentrations, LY290181 affected mitotic spindle microtubules in the absence of massive depolymerization of microtubules.

Inhibition of microtubule assembly by LY290181. Based upon the foregoing results in cells, it appeared that

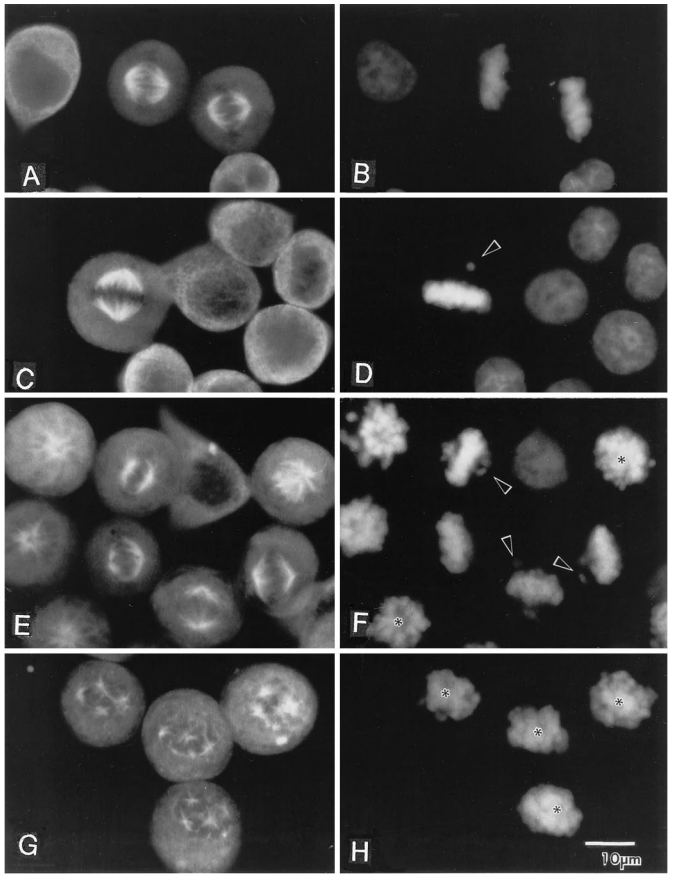

Fig. 5. Effect of LY290181 on mitosis and spindle microtubules. HeLa cells were incubated with LY290181 for 20 hr. Spindle microtubule (A, C, E, and G) and chromosome (B, D, F, and H) were investigated. A and B, Two spindles in control cells with well defined compact metaphase plate of chromosome. C and D, LY290181 (3 nM), abnormal bipolar spindle with one uncongressed chromosome at one spindle pole (*arrowhead*) and several cells in interphase. E and F, LY290181 (10 nM), many cells are in mitosis, spindles appear normal as well abnormal and bipolar with uncongressed chromosomes (*arrowhead*) or have ball-shaped aggregates of chromosomes (*). G and H, LY290181 (30 nM), most cells are in mitosis; spindle are bass-shaped with small star-shaped array of short microtubules.

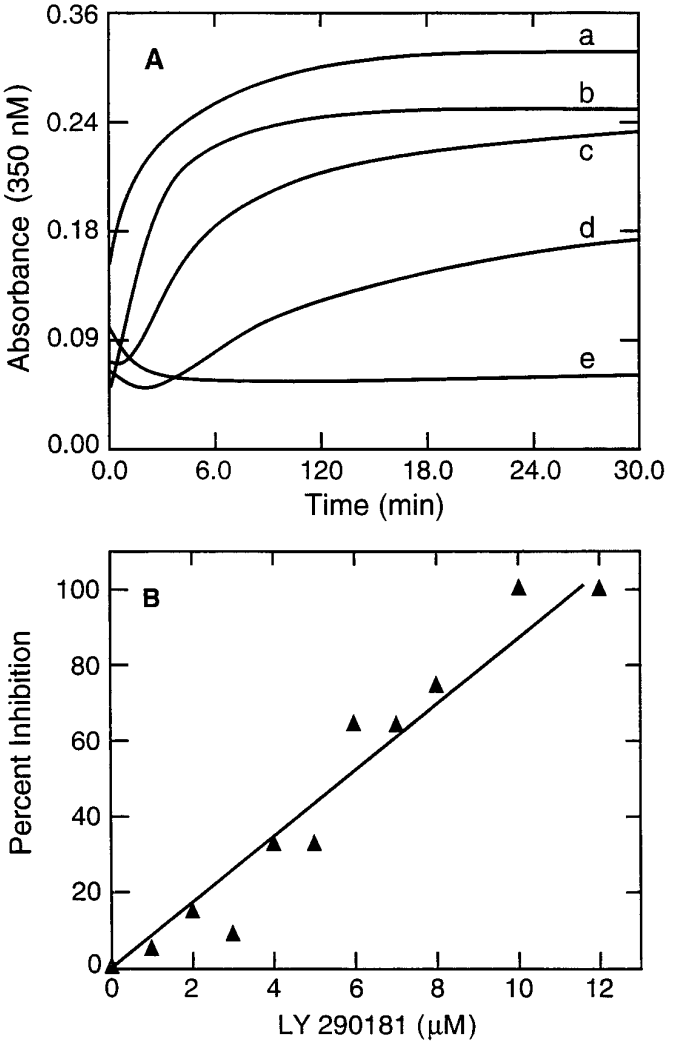

Fig. 6. Inhibition of microtubule polymerization by LY290181. A, Polymerization of microtubule protein (1.2 mg/ml) in the absence (*a*) or presence of 2 μM (*b*), 4 μM (*c*), 6 μM (*d*), and 10 μM (*e*) LY290181 was determined at 350 nm. B, Inhibition of microtubule polymerization at 30 min (plateau) is plotted as a function of LY290181 concentration. Data are representative of three experiments. The line represents a linear fit of the data.

LY290181 was exerting its antiproliferative effects by affecting microtubule structure and function. In support of these findings, we further showed that LY290181 could inhibit the polymerization of bovine brain microtubule protein into microtubules *in vitro*. Fig. 6A shows that LY290181 produced a concentration dependent inhibition of the rate and extent of microtubule polymerization. Inhibition of tubulin polymerization by LY290181 as a function of LY290181 concentration is shown in Fig. 6B. Fifty percent inhibition (IC_{50}) was achieved at 5.5 μM.

We also determined the effect of LY290181 on preformed microtubules. Addition of 10 μM LY290181 to a suspension of microtubules made from microtubule protein (MAPs plus tubulin) induced a rapid disassembly of the microtubules (within ~10 min of drug addition). Video microscopic studies also showed that LY290181 (2 μM) produced extensive depolymerization of axoneme-seeded microtubules prepared from phosphocellulose-purified tubulin (19) (data not shown). These results demonstrate that LY290181 inhibits microtubule polymerization and induces depolymerization of preformed microtubules.

Direct interaction of LY290181 with tubulin at a novel site. The apolar molecule ANS stoichiometrically binds to tubulin at a single site (17). The ANS binding sites in tubulin do not overlap with the binding sites for colchicine, podophyllotoxin, vinblastine, or maytansine (17). The tubulin-ANS complex fluoresces strongly, making it a useful tool for probing conformational states of the tubulin dimer (17, 18). We have used tubulin-ANS fluorescence to determine the direct interaction of LY290181 with tubulin and to determine the nature of the binding site. Tubulin (2 μM) was incubated with a range of concentrations of LY290181 for 30 min at 34° in 50 mM PEM buffer. ANS (50 μM) was added to the tubulin-LY290181 complex, and the incubation was continued for an additional 15 min. Fig. 7A shows that LY290181 produced a concentration-dependent decrease in tubulin-ANS fluorescence. Half-maximal reduction occurred at 2.9 μM LY290181.

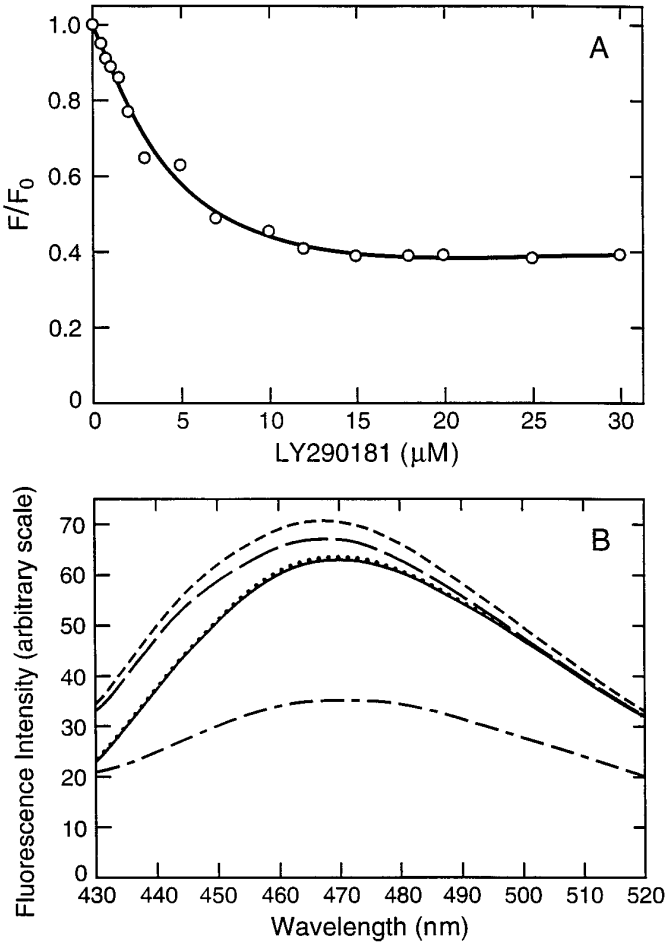

Fig. 7. Reduction of tubulin-ANS complex fluorescence by LY290181. *A*, Tubulin (2 μM) was mixed with the indicated concentrations of LY290181 for 30 min at 34°. ANS (50 μM) was then added and fluorescence was measured after 15 min of incubation. The excitation and emission wavelengths were 400 and 468 nm, respectively. B, Fluorescence in control (—), in the presence of 22 μM LY290181 (- — —), 25 μM vinblastine (- - -), 25 μM nocodazole (···) or 25 μM podophyllotoxin (— —).

Furthermore, incubation of tubulin with ANS before the addition of LY290181 produced similar results (data not shown). The strong reduction in fluorescence of the tubulin-ANS complex by LY290181 may result from the binding of ANS and LY290181 to the same region of tubulin. Alternatively, LY290181 binding to tubulin may induce a conformational change in tubulin leading to the reduction in ANS binding or tubulin-ANS fluorescence. These data demonstrate that LY290181 binds strongly to the tubulin dimer.

We also compared the effect of LY290181 on ANS-tubulin fluorescence with known tubulin-binding agents. As shown in Fig. 7B, under identical conditions, LY290181 strongly reduced tubulin-ANS fluorescence, whereas vinblastine enhanced and nocodazole and podophyllotoxin had no effect on the fluorescence intensity. These results indicate that LY290181 induces a unique conformational change in tubulin. Together with our recent studies (13), these data suggest that LY290181 inhibits cell proliferation by binding to a novel site in tubulin and suppressing dynamics of mitotic spindle microtubules.

Discussion

In the present study, we have found that LY290181 is a potent inhibitor of proliferation of rabbit smooth muscle cells, CHO cells, endothelial cells, HeLa cells, and erythroleukemia cells. The IC_{50} for cell growth inhibition was in the range of 10–40 nM. Determination of DNA synthesis in density-arrested quiescent smooth muscle cells induced to progress from G_0/G_1 to S phase showed that a 15-fold higher concentration of LY290181 was required for inhibition of DNA synthesis than for inhibition of cell proliferation (data not shown). These results suggest that the predominant action of LY290181 occurs at stages other than the G_1 or S phase of the cell cycle.

Using fluorescence activated cell sorting and cell cycle analysis, we found that LY290181 produced a selective accumulation of smooth muscle cells in the G_2/M phase of the cell cycle. In cultures treated with 30 or 100 nM LY290181, 28.9 and 68.6% of the cells, respectively, accumulated in G_2/M phase as compared with 16.8% of the cells in control cultures. The increase in G_2/M cells was accompanied by a decrease in G_0/G_1 cells. Mitotic index determination of cycling CHO cells and HeLa cells also showed that LY290181 induced an accumulation of cells in mitosis in a concentration-dependent manner and that accumulation of cells at mitosis correlated with the concentration response for cell growth inhibition by the compound. Thus, the results of FACS and mitotic index studies indicate that LY290181 inhibited cell cycle progression at mitosis. Further examination of chromosomal and microtubule morphology of CHO cells and HeLa cells during mitosis indicated that LY290181 selectively inhibited cell cycle progression at prometaphase/metaphase.

Examination of microtubule organization by FITC-conjugated tubulin antibody staining showed that at low concentrations, including that required for 50% inhibition of cell proliferation (30 nM), LY290181 did not produce a discernible change in the organization of interphase cytoplasmic microtubules (Fig. 4). At higher concentrations, LY290181 produced a concentration-dependent disruption of the cytoplasmic microtubules, and a clear reduction in polymer density. Microtubule staining in the cytoplasm was dramatically reduced at concentrations >100 nM LY290181 leading to a near complete loss of microtubule staining at 500 nM. Similarly, low concentrations (≤30 nM) of LY290181 produced abnormal organization of mitotic spindle microtubules in HeLa cells. At high concentrations (≥100 nM), LY290181 produced depolymerization of spindle microtubules.

A notable difference in the action of LY290181 on microtubules as compared with the actions of vinblastine and Taxol was that unlike vinblastine and Taxol, high concentrations of LY290181 did not induce microtubule bundling or tubulin paracrystal formation (20). This may suggest a distinct mode of interaction of LY290181 with microtubules from vinblastine and Taxol. Although high concentrations of LY290181 induced microtubule depolymerization, a significant loss of cytoplasmic microtubules occurred at about 2-fold higher LY290181 concentration than that required for 50% inhibition of cell growth in CHO cells. Thus, gross depolymerization of cytoplasmic microtubules does not appear to be associated with cell growth inhibition by LY290181. Instead, subtle effects on microtubule dynamics may be a more relevant mechanism for its antiproliferative action.

Based on its effects on microtubule organization in intact cells, we investigated whether LY290181 directly affected microtubule polymerization. Using isolated bovine brain microtubule protein consisting of tubulin and MAPs, we found that LY290181 inhibited both the rate and extent of microtubule assembly *in vitro*. The concentration of LY290181 required for 50% inhibition of microtubule polymerization was 5.5 μM. The potency of LY290181 was comparable to known anti-microtubule compounds such as colchicine or vinblastine (20). Both turbidimetric and video microscopic studies showed that LY290181 also induces depolymerization of preformed microtubules (data not shown).

Using ANS-tubulin complex fluorescence, we found that LY290181 directly interacted with tubulin. The reduction in tubulin-ANS fluorescence may imply that LY290181 binds to the same region of tubulin as ANS or that it produces a conformational change that affects ANS binding or fluorescence. Our studies also show that the ability of LY290181 to reduce ANS-tubulin complex fluorescence was unique and distinct from vinblastine, nocodazole, and podophyllotoxin. These data suggest that the tubulin binding site for LY290181 may be different from the above antimitotic agents.

In summary, the depolymerization of cytoplasmic microtubules by high concentrations of LY290181 in cells and *in vitro* the alteration of spindle organization by low concentration of LY290181 and its direct effect on tubulin-ANS fluorescence have provided strong evidence suggesting that microtubules and tubulin are the molecular targets for LY290181. We have recently demonstrated that the LY290181 kinetically stabilizes microtubule dynamics (13). These results suggest that LY290181 inhibits cell proliferation by stabilizing spindle microtubule dynamics. Because microtubule functions are essential for cell division, cell movement, cell adhesion, and cell spreading, interference with microtubule dynamics may offer a potential treatment modality for proliferative disease such as restenosis and neoplasia. Proliferation and migration of vascular smooth muscle cells play a critical role in vascular remodeling after vascular injury (1, 21). Agents inhibiting vascular smooth muscle cell proliferation and migration effectively block intimal thickening in vascular injury models (7–10, 22–24). Anti-microtubule drugs have proven to be effective therapy for the treatment for several types of malignancies. Recent studies have shown that the microtubule-stabilizing drug Taxol reduces intimal thickening in a rat model of balloon-induced vascular injury (25). The plasma concentrations of Taxol, at doses effective for the reduction in intimal thickening, were 10–1000-fold lower than the peak concentration achieved for anti-cancer efficacy (25, 26). Furthermore, the concentrations of taxol needed for the inhibition of intimal thickening were significantly below the cytotoxicity range for Taxol (25, 26). These early studies on microtubule modulating compounds are encouraging with regard to their potential use in the treatment of restenosis. Our previous studies have shown that LY290181 administered either orally or subcutaneously produced significant reduction in intimal thickening in a rat carotid artery injury model (10). Because the concentrations of LY290181 required to produce antiproliferative and antimigration actions are significantly lower than that required for depolymerization of cytoplasmic microtubules, the use of lower concentrations of the compound may allow selective inhibition of cell proliferation and migration *in vivo*.

Acknowledgments

We wish to thank Philip Marder and Larry Mann for assistance in FACS analysis and Keith Deluca for expert technical assistance.

References

1. Ross R. The pathogenesis of atherosclerosis: a perspective for the 1990s. *Nature (Lond.)* **362:**801–809 (1993).
2. Schoen, F. J., and P. Libby. Cardiac transplant graft arteriosclerosis. *Trends. Cardiovasc. Med.* **1:**216–223 (1991).
3. Isner, J. M., M. Kearianne, C. Bauters, G. Leclerc, S. Nikol, G. Pickering, R. Riessen, and L. Weir. Use of human specimens obtained by directional atherectomy to study restenosis. *Trends Cardiovasc. Med.* **4:**213–221 (1994).
4. Heagerty, A. M., C. Aalkjaer, S. J. Bund, N. Korsgaard, and M. J. Mulvany. Small artery structure in hypertension: dual process of remodeling and growth. *Hypertension (Dallas)* **21:**391–397 (1993).
5. Rekhter, M., S. Nicholis, M. Ferguson, and D. Gordon. Cell proliferation in human arteriovenous fistulas used for hemodialysis. *Arterioscler. Thromb.* **13:** 609–617 (1993).
6. D'Amico D. J. Disease of the retina. *N. Engl. J. Med.* **331:**95–106 (1994).
7. Casscells, W., D. A. Lappi, B. B. Olwin, C. Wai, M. Siegman, E. H. Speir, J. Sasse, and A. Baird. Elimination of smooth muscle cells in experimental restenosis: targeting of fibroblast growth factor receptor. *Proc. Natl. Acad. Sci. USA* **89:**7159–7163 (1992).
8. Bennett, M. R., S. Anglin, J. R. McEwan, R. Jagoe, A. C. Newby, and G. I. Evan. Inhibition of vascular smooth muscle cell proliferation in vitro and in vivo by c-*myc* antisense oligodeoxynucleotides. *J. Clin. Invest.* **93:**820–828 (1994).
9. Simons, M., E. R. Edelman, J. DeKeyser, R. Langer, and R. Rosenberg. Antisense c-*myb* oligodeoxynucleotides inhibit arterial smooth muscle accumulation in vivo. *Nature (Lond.)* **359:**67–70 (1992).
10. Wiernicki, T. R., J. S. Bean, D. Dell, A. Williams, D. Wood, R. F. Kauffman, and J. P. Singh. Inhibtion of vascular smooth muscle cell proliferation and arterial intimal thickening by a novel antiproliferative naphthopyran. *J. Pharmacol. Exp. Ther.* **278:**1452–1459 (1996).
11. Chandrasekhar, S., A. K. Harvey, C. P. Dell, S. J. Ambler, C. W. Smith. Identification of a novel chemical series that blocks interleukin-1 stimulated metalloprotease activity in chondrocytes. *J. Pharmacol. Exp. Ther.* **273:**1519–1528 (1995).
12. Birch, K. A., W. F. Heath, R. N. Hermling, C. M. Johnston, L. Stramm, C. Dell, C. Smith, J. R. Williamson, A. R. Miller. LY290181, an inhibitor of diabetes-induced vascular dysfunction, blocks protein kinase C-stimulated transcription factor binding to phorbol response element. *Diabetes* **45:**642–650 (1996).
13. Panda, D., J. P Singh, and L. Wilson. Suppression of microtubule dynamics by LY290181. A potential mechanism for its antiproliferative action. *J. Biol. Chem.* **272:**7681–7687 (1997).
14. Arevalo, M. A., J. M. Nieta, D. Andreu, and J. M. Andreu. Tubulin assembly probed with antibodies to synthetic peptides. *J. Mol. Biol.* **214:**105–120 (1990).
15. Jordan, M. A., D. Thrower, and L. Wilson. Effect of vinblastine, podophyllotoxin and nocodazole on mitotic spindles, implications for the role of microtubules dynamics in mitosis. *J. Cell Sci.* **102:**401–416 (1992).
16. Toso, R. J., M. A. Jordan, K. W. Farrell, B. Matsumoto, and L. Wilson. Kinetics stabilization of microtubules dynamic instability in vitro by vinblastine. *Biochemistry* **32:**1285–12931 (993).
17. Bhattacharya, B., and J. Wolff. The interaction of 1-Anilino-8-naphthalene sulphonate with tubulin: a site independent of colchicine binding site. *Arch. Biochem. Biophys.* **167:**264–269 (1975).
18. Lee, J. C., D. Harrison, and S. N. Timasheff. Interaction of vinblastine with calf brain microtubule protein. *J. Biol. Chem.* **250:**9276–9282 (1975).
19. Panda, D., B. L. Good, S. C. Feinstein, and L. Wilson. Kinetic stabilization of microtubule dynamics at steady state by tau and microtubule-binding domains of tau. *Biochemistry* **34:**11117–11127 (1995).
20. Hamel, E. Interactions of tubulin with small ligands, in *Microtubule Proteins* (J. A. De Grado ed.). CRC Press, Boca Raton, FL, 88–191 (1989).
21. Lee, P. C., G. H. Gibbons, and V. J. Dzau. Cellular and molecular mechanisms of coronary artery restenosis. *Coron. Artery Dis.* **4:**254–259 (1993).
22. Guzman, R. J., E. A. Hirschowitz, S. L. Brody, R. G. Crystal, S. E. Epstein, and T. Finkel. In vivo suppression of injury-induced vascular smooth muscle cell accumulation using adenovirus-mediated transfer of the herpes simplex virus thymidine kinase gene. *Proc. Natl. Acad. Sci. USA* **91:**10732–10736 (1994).
23. Maresta, A., M. Balducelli, L. Cantini, A. Casari, R. Chioin, M. Fabbri, A. Fontanelli, P. A. Monici Preti, S. Repelto, S. De Servi, et al. Trapidil (triazolopyrimidine), a platelet-derived growth factor antagonist, reduces

restenosis after percutaneous transluminal coronary angioplasty. *Circulation* **90:** 2710–2715 (1994).
24. Morishita, R., G. H. Gibbons, K. E. Ellison, M. Nakajima, H. Leyen, L. Zhang, Y. Kaneda, T. Ogihara, and V. Dzau. Intimal hyperplasia after injury is inhibited by antisense cdK2 kinase oligonucleotides. *J. Clin. Invest.* **93:**1458–1464 (1994).
25. Sollott, S. J., L. Cheng, R. R. Pauly, G. M. Jenkins, R. E. Monticone, M. Kuzuya, J. P. Froehlich, M. T. Crow, E. G. Lakatta, E. K. Rowinsky, and J. L. Kinsella. Taxol inhibits neointimal smooth muscle cell accumulation after angioplasty in the rat. *J. Clin. Invest.* **95:**1869–1876 (1995).
26. Huizing, M. T., A. C. Keung, H. Rosing, V. Kuij, B. Huinink, I. M. Masndjes, A. C. Dubbelman, and J. H. Beijnen. Pharmacokinetics of paclitaxel and metabolites in a randomized comparative study in platinum-pretreated ovarian cancer patients. *J. Clin. Oncol.* **11:**2127–2135 (1993).

Send reprint requests to: Dr. Jai Pal Singh, Lilly Research Laboratories, DC 0520, Indianapolis, IN 46285.